

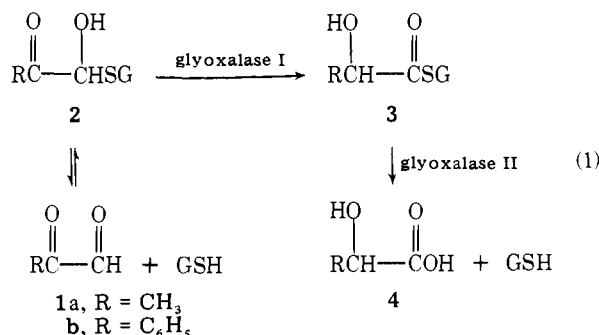
# Glyoxalase I Enzyme Studies.<sup>1</sup> 4.<sup>2</sup> General Base Catalyzed Enediol Proton Transfer Rearrangement of Methyl- and Phenylglyoxalglutathionylhemithiol Acetal to *S*-Lactoyl- and *S*-Mandeloylglutathione Followed by Hydrolysis. A Model for the Glyoxalase Enzyme System

Stan S. Hall,\* Arthur M. Doweyko,<sup>3</sup> and Frank Jordan\*

Contribution from the Carl A. Olson Chemistry Laboratories, Department of Chemistry, Rutgers University, Newark, New Jersey 07102. Received November 14, 1977

**Abstract:** In the presence of the general bases imidazole and phosphate dianion methyl- and phenylglyoxalglutathionylhemithiol acetals rearrange to the corresponding *S*-lactoyl- and *S*-mandeloylglutathiones, respectively, and then hydrolyze to the corresponding acids. NMR-detected incorporation of solvent protons indicates the mechanism of the arrangement to be an enediol proton transfer. The essential catalytic components of the reaction, which with respect to the mechanism is a bona fide model for the enzyme glyoxalase I, are the covalent catalyst glutathione (the coenzyme for the enzymatic process) and a general base. The rate is also enhanced slightly by magnesium ions. The magnitude of the primary kinetic isotope effect for the general base catalyzed reaction is smaller than that for the hydroxide ion (Cannizzaro) catalyzed rearrangement that involves an intramolecular 1,2-hydride shift mechanism. Reexamination of Franzen's model reaction using NMR techniques indicates that the *N,N*-diethylcysteamine catalyzed rearrangement also proceeds via an enediol proton transfer rather than a 1,2-hydride shift.

The glyoxalase enzyme system consisting of glyoxalase I [*S*-lactoyl-glutathione methylglyoxal-lyase (isomerizing) E.C. 4.4.1.5], the coenzyme glutathione (GSH), and glyoxalase II (*S*-2-hydroxyacylglutathione hydrolase, E.C. 3.1.2.6) converts methylglyoxal (**1a**) and phenylglyoxal (**1b**) to lactic acid (**4a**) and mandelic acid (**4b**), respectively. Recent suggestions and evidence that glyoxalase I and its substrate may be essential controlling factors in the regulation of cell division<sup>4</sup> have rekindled interest in this enzyme system and its mechanism.



Mechanistically, the most interesting step in the reaction sequence is the glyoxalase I catalyzed rearrangement of the hemithiol acetal **2** to the thiol ester **3**. Results of solvent (deuterium oxide<sup>5</sup> and tritium-enriched water<sup>6</sup>) incorporation studies led earlier investigators to conclude that the mechanism proceeds via an intramolecular hydride shift. However, recent high-resolution NMR evidence presented by this laboratory indicated low incorporation of solvent protons (from deuterium oxide) to form [2-<sup>2</sup>H]lactic acid. This observation of incorporation, which also increased as the temperature was raised, suggests a fast-shielded enediol proton transfer that is occurring at a highly protected active site.<sup>2a</sup> In addition, such a mechanism suggests the participation of a basic amino acid residue at the active site.<sup>7</sup>

Heretofore, nonenzymatic catalysts that have mimicked the enzymic reaction include Franzen's use of 2-dialkylaminoethanethiols;<sup>5,8</sup> our magnesium ion-base catalyzed rear-

rangement of *S*-alkyl  $\alpha$ -ketoemithiol acetals to  $\alpha$ -hydroxythiol esters with such bases as sodium acetate or *N*-methylpyrrolidine in aqueous dimethylformamide solutions;<sup>9</sup> Hine and Koser's studies on the hydroxide catalyzed rearrangement of phenylglyoxal to mandelic acid;<sup>10</sup> and most recently Hine and Fischer's *N,N,N'*-trimethylethylenediamine internal catalyzed conversion of phenylglyoxal to the corresponding mandelamide derivative.<sup>11</sup> The model study reported herein was initiated to examine the potential conversion of  $\alpha$ -ketoaldehydes to  $\alpha$ -hydroxy acids in the presence of the apparently essential catalytic components of the enzyme. These would include glutathione along with magnesium ion<sup>9,12</sup> and a base<sup>7,9</sup> (imidazole and phosphate dianion were examined) rather than glyoxalase I holoenzyme in its role as *deus ex machina*. In addition, the question of an intramolecular 1,2-hydride shift vs. an enediol proton transfer mechanism for this model study was examined and the model of Franzen,<sup>5,8</sup> on which many of the previous conclusions about the enzyme mechanism have been based, reexamined.

## Results and Discussion

**General Base Catalysis.** The choice of bases investigated as potential general base catalysts was guided by several factors. The broad optimum pH range (5-9) observed for glyoxalase I activity<sup>13</sup> would suggest model studies in this pH range. Of the common amino acid residues with pK values in this pH range,<sup>14</sup> those containing primary amines and thiols were not considered since they might also lead to the formation of nucleophilic adducts with the  $\alpha$ -ketoaldehydes. Of the remaining possibilities, the aromatic amine imidazole (pK 6.95) was found to be a catalyst in this rearrangement of the hemithiol acetal **2** to the thiol ester **3**. Phosphate dianion, with a similar pK, was also found effective. The  $K_{\text{diss}}$  for the equilibrium between **1a** and **2a** has been determined to be  $3 \times 10^{-3}$  M.<sup>4d,15</sup>

**HPO<sub>4</sub><sup>2-</sup> Catalysis.** The basic form of the buffer was shown to be the catalytically active species by the following experiments. While maintaining a 0.1 M total phosphate solution with a constant ionic strength of 0.4 by adding KCl, the mole fraction of H<sub>2</sub>PO<sub>4</sub><sup>-</sup>/HPO<sub>4</sub><sup>2-</sup> was varied by adjusting the pH.

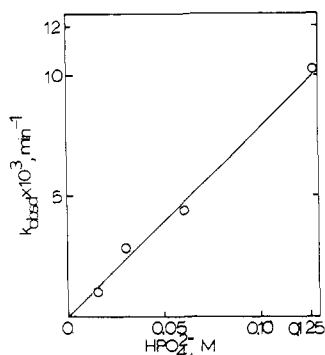


**Figure 1.** Dependence of  $k_{\text{obsd}}$  on total phosphate dianion concentration at pH 7.0 and 30 °C. Ionic strength was maintained at 0.4 (KCl).

It was found that the pseudo-first-order rate constant varied linearly with  $\text{HPO}_4^{2-}$  concentration and extrapolated to a zero rate constant at zero  $\text{HPO}_4^{2-}$  concentration. Significant catalysis by either  $\text{H}_2\text{PO}_4^-$  or  $\text{H}_2\text{O}$  can be ruled out. Figure 1 shows the dependence of  $k_{\text{obsd}}$  on  $\text{HPO}_4^{2-}$  concentration at a constant pH of 7.00. Within experimental error, the catalysis is due solely to the buffer. From the slope, the value of  $(8.0 \pm 0.9) \times 10^{-2} \text{ M}^{-1} \text{ min}^{-1}$  for the second-order rate constant  $k_{\text{HPO}_4^{2-}}$  was obtained.

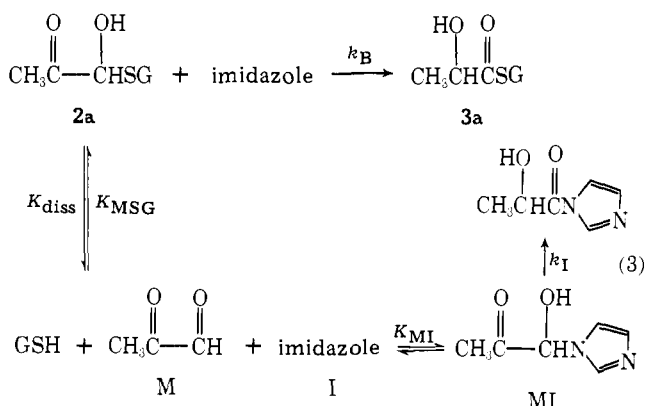
**Imidazole Catalysis.** The source of catalysis by imidazole was examined by varying the imidazole/imidazolium ratio while keeping the total concentration constant. The results at total buffer concentrations of 0.20 and 0.35 M indicated the basic form of the buffer (imidazole) to be the exclusive catalytic agent.

At pH 7.0 the plot of  $k_{\text{obsd}}$  vs. imidazole (neutral) concentration became nonlinear (downward curvature) at concentrations exceeding 0.2 M. The simple rate expression:

$$\text{rate} = \frac{-d[\text{CH}_3\text{C}(=\text{O})\text{C}(\text{OH})\text{HSG}]}{dt} = k_B[\text{CH}_3\text{C}(=\text{O})\text{C}(\text{OH})\text{HSG}][\text{B}] \quad (2)$$

could no longer be utilized to obtain  $k_B$  for imidazole. In order to analyze this behavior we assumed that imidazole could interact as well with the aldehyde to form the addition product MI that, by analogy to previous studies with secondary amines,<sup>11</sup> might rearrange slowly to *N*-lactoylimidazole.

In the Appendix we show a derivation allowing determination of  $K_{\text{MI}}$  as  $12.9 \pm 2.3 \text{ M}^{-1}$ . Qualitatively, such competition would reduce the concentration of hemithiol acetal **2a** available for rearrangement to **3a**. Assuming the only reaction pathways are those outlined in eq 3 and the hemiimidazole acetal (MI)



rearranges at a much slower rate ( $k_I \ll k_B$ ) than the hemithiol acetal **2a**, the quantitative effects of this competing reaction can be predicted. Since

$$[\text{M}]_0 = [\text{M}] + [\text{MSG}] + [\text{MI}] \quad (4)$$

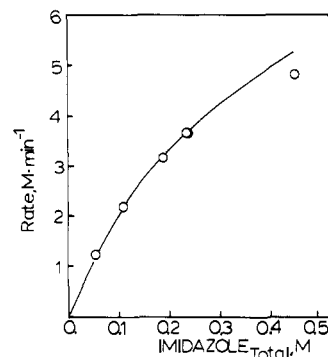


**Figure 2.** Comparison of experimental rates with calculated values for the imidazole catalyzed reactions at pH 7.0 assuming the scheme in eq 3 (see derivation in Appendix). The solid line represents the calculated and the circles the observed values.

and then substituting equilibrium constants into the equation

$$[\text{M}]_0 = [\text{M}] \left( 1 + \frac{K_{\text{MSG}} [\text{GSH}]}{1 + K_{\text{MSG}} [\text{M}]} + \frac{K_{\text{MI}} [\text{I}]_0}{1 + K_{\text{MI}} [\text{M}]} \right) \quad (5)$$

By successive approximations  $[\text{M}]$  and hence  $[\text{MSG}]$  could be determined for each  $[\text{I}]_0$ . Knowledge of  $[\text{MSG}]$  allowed determination of the second-order rate constant  $k_B$  in eq 3 for imidazole as  $5.5 \times 10^{-2} \text{ M}^{-1} \text{ min}^{-1}$ .<sup>16</sup> Figure 2 presents calculated and observed rate data based on these assumptions. The agreement, especially at low imidazole concentrations, is satisfactory. Hine and Fischer recently measured association constants between secondary amines and phenylglyoxal (**1b**) and obtained values of 20–100  $\text{M}^{-1}$ .<sup>11</sup> Thus, the assumption that imidazole associates with methylglyoxal (**1a**) and the values suggested here for this association ( $K_{\text{MI}}$  as  $12.9 \pm 2.3 \text{ M}^{-1}$ ) appear to be of the right order of magnitude. Although we have no evidence at present as to whether the hemiimidazole acetal rearranges to *N*-lactoylimidazole, Figure 2 in fact suggests that it does not since the predicted rate should be lower than that observed if  $k_I[\text{MI}]$  were making a significant contribution to the overall rate. In addition, the freshly prepared solutions of methylglyoxal and imidazole employed in the determination of  $K_{\text{MI}}$  above did not change in absorbance over several hours, suggesting that no rearrangement was occurring.

**Effect of Magnesium Ions.** It has been known for some time that glyoxalase I contains a tightly bound magnesium ion that is essential for enzymatic activity.<sup>12</sup> In previous model studies in a nonaqueous system (DMF) with tertiary amines and sodium acetate as bases, a 30-fold acceleration of the reaction rate was observed by adding magnesium ions.<sup>9a</sup> However, in the present model study in aqueous medium using imidazole as the base, the rate of the rearrangement was accelerated by only a factor of 1.8.<sup>9b</sup> We attribute much of the diminished effect of the magnesium ions to the competing complexing of the ions to imidazole and water.

**Deuterium Isotope Effects.** Having observed general base catalysis in the rearrangement of the  $\alpha$ -keto-hemithiol acetal **2** to the  $\alpha$ -hydroxythiol ester **3**, it was of interest to measure the magnitude of the isotope effect on this reaction by substituting deuterium for hydrogen at the C-1 position of the  $\alpha$ -ketoaldehyde **1**. This general base catalyzed pathway, which proceeds by an enediol mechanism (see below), gave rise to a kinetic isotope effect of  $3.3 \pm 0.5$  for  $\text{CH}_3\text{COCHO}$  vs.  $\text{CD}_3\text{COCHO}$  and  $2.3 \pm 0.2$  for  $\text{C}_6\text{H}_5\text{COCHO}$  vs.  $\text{C}_6\text{D}_5\text{COCHO}$ . These numbers are consistently lower than those obtained in the hydroxide ion catalyzed reaction (internal Cannizzaro involving a 1,2-hydride shift mechanism) of 3.8 for the methylglyoxals and 5.0 for the phenylglyoxals.<sup>13b</sup> The

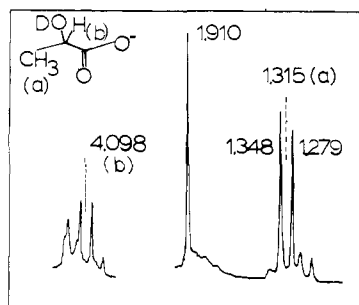


Figure 3. Part of the  $^1\text{H}$  NMR spectrum of the  $\text{KH}_2\text{PO}_4$  catalyzed conversion of methylglyoxal to lactic acid in  $\text{H}_2\text{O}$ . Chemical shifts are quoted in parts per million from DSS.

magnitudes of the primary kinetic  $^2\text{H}$  isotope effects obtained with the above substrates reported as  $V_{\max}(^1\text{H})/V_{\max}(^2\text{H})$  for the enzyme-catalyzed reaction vary widely depending on the source of the enzyme. With methylglyoxal as substrate, the value for the enzyme isolated from yeast was  $2.9 \pm 0.2^{13b}$  and values ranged from 1.0 to 3.5, depending on the metal ion, with the enzyme isolated from rat erythrocyte.<sup>17</sup> Using phenylglyoxal as substrate, the value for the yeast enzyme was  $3.2 \pm 0.3^{13b}$  and values ranging from 2.1 to 4.8 were obtained with the rat erythrocyte enzyme,<sup>17</sup> again depending on the metal employed.

For the model systems, the magnitudes of the primary kinetic  $^2\text{H}$  isotope effects appear to be characteristic of the type of mechanism and thus seem to differentiate the enediol proton transfer from the 1,2-hydride shift. With the enzyme, however,  $V_{\max}(^1\text{H})/V_{\max}(^2\text{H})$  at best indicates only that the hydrogen transfer is rate limiting but does not distinguish the nature of the hydrogen transfer. It is interesting to note that the magnitude of the isotope effect reported here for the general base catalyzed (enediol) mechanism is similar to the value of 2.9 recently observed for triosephosphate isomerase.<sup>18</sup> This enzymatic process involves proton abstraction from the substrate 1(*R*)-dihydroxyacetone phosphate and generates an enediol intermediate.

**Mechanistic NMR Studies.** Mechanistically, the most intriguing step in the reaction sequence is the rearrangement of the hemithiol acetal **2** to the  $\alpha$ -hydroxythiol ester **3** for which one might consider either an intramolecular 1,2-hydride shift (intramolecular Cannizzaro) or an enediol proton transfer mechanism. Distinguishing the two mechanisms is straightforward with NMR either by detecting the incorporation (or lack of incorporation) of solvent protons into the product or the retention (or loss to the medium) of an isotope of hydrogen when using a properly labeled substrate. We have previously used both incorporation of solvent and loss of deuterium to the medium in studies that established that the enzymatic reaction proceeds via a fast-shielded enediol proton transfer that is occurring at a highly protected active site.<sup>2a</sup> In addition, solvent incorporation studies indicated that the magnesium ion-base catalyzed rearrangement of *S*-alkyl  $\alpha$ -keto-hemithiol acetals to  $\alpha$ -hydroxythiol esters in  $\text{D}_2\text{O}$ -DMF also proceeds by an enediol proton transfer mechanism.<sup>9</sup> Consequently, it was important to determine the mechanism of the enzymatic model study reported here, as well as to reexamine Franzen's model system, for which a 1,2-hydride shift mechanism had been proposed,<sup>5,8</sup> using NMR techniques.

If the model reaction is run in  $\text{D}_2\text{O}$  using methylglyoxal (**1a**) as substrate, either lactic acid (product of a 1,2-hydride shift) or  $[2\text{-}^2\text{H}]$ lactic acid (product of an enediol proton transfer) will be the product depending on the mechanism.

Figure 3 shows part of the 100-MHz  $^1\text{H}$  NMR spectrum of the model reaction catalyzed by  $\text{KH}_2\text{PO}_4$  in  $\text{H}_2\text{O}$  and indicates that lactic acid is formed. The spectrum is superim-

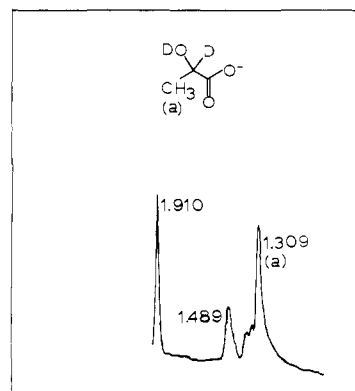


Figure 4. Part of the  $^1\text{H}$  NMR spectrum of the  $\text{KH}_2\text{PO}_4$  catalyzed conversion of methylglyoxal to  $[2\text{-}^2\text{H}]$ lactic acid in  $\text{D}_2\text{O}$ . Chemical shifts are quoted in parts per million from DSS.

posable with that of an authentic sample of lactic acid.

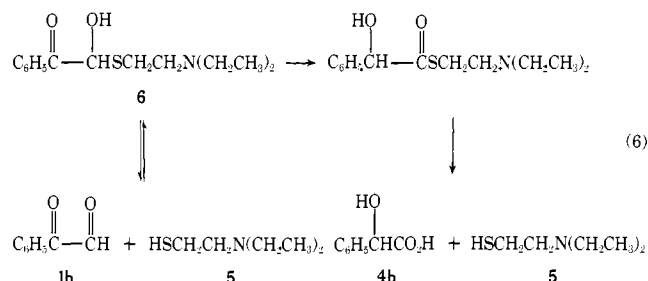
Before any firm conclusions can be drawn about the model system with regard to the question of solvent incorporation, it is necessary to establish that none of the compounds **1**, **2**, **3**, or **4** in eq 1 incorporates solvent protons when exposed to these conditions. Compounds **1**, **2**, and **4** have been repeatedly tested in this and related studies<sup>2a,9</sup> and do not exchange protons with the medium. This then leaves the possibility that the thiol ester **3** rapidly incorporates solvent protons as soon as it is formed. The latter possibility could be eliminated in a control experiment using the enzyme as catalyst as follows. *S*-Lactoylglutathione (**3a**) was formed by the conversion of the hemithiol acetal **2a** with glyoxalase I in  $\text{D}_2\text{O}$  buffered with  $\text{KH}_2\text{PO}_4$ . Under these conditions very little incorporation occurs.<sup>2a</sup> In the 100-MHz NMR spectrum of the thiol ester **3a**, the methyl region of the lactoyl group is a large doublet centered at 1.368 ppm ( $J = 6.8$  Hz, peaks at 1.333 and 1.403 ppm) for the unincorporated thiol ester that is superimposed on a much smaller singlet (shoulder) at 1.364 ppm for the incorporated thiol ester. These relative areas for the methyl group did not change with respect to each other (the doublet vis-a-vis the singlet) nor with respect to the intensity of the DSS signal when this enzymatic reaction mixture was monitored for ca 8 h at 28 °C (after ca. 24 h some hydrolysis was evident) or after heating at 84 °C for 10 min. Subsequent addition of solid KOH led to immediate hydrolysis of the thiol ester **3a** to lactate with an intense doublet centered at 1.315 ppm ( $J = 6.9$  Hz, peaks at 1.279 and 1.348 ppm) and a small singlet at 1.309 ppm. The ratio of the doublet, the singlet, and DSS was within detection limits, the same as that of the doublet, the singlet, and DSS of the thiol ester. This experimental sequence demonstrates that the thiol ester **3a** does not exchange the hydrogen at the  $\alpha$  position during these or more severe reaction conditions, and that specific base-catalyzed hydrolysis of the thiol ester **3a** to lactic acid (**4a**) results in no incorporation of solvent protons into the  $\alpha$  position. If incorporation occurs when the model reaction is carried out in  $\text{D}_2\text{O}$ , then it must be incorporated during the conversion of hemithiol acetal **2a** to thiol ester **3a**.

Figure 4 displays part of the 100-MHz  $^1\text{H}$  NMR spectrum of the final hydrolysis product of the model reaction that was carried out in buffered  $\text{D}_2\text{O}$  at pD 7.40. Clearly the methyl doublet for lactic acid centered at 1.315 ppm has now collapsed to an apparent singlet centered at 1.309 ppm, which is coincident with a spectrum of authentically prepared  $[2\text{-}^2\text{H}]$ lactic acid. An incorporation of at least 90% is evident. Prior to hydrolysis the intermediate thiol ester **3a** could also be observed by  $^1\text{H}$  NMR. An apparent singlet centered at 1.364 ppm for the lactoyl methyl group indicated that incorporation had already occurred. These observations, in conjunction with the controls described above, demonstrate an enediol proton

transfer mechanism for the model reaction.

As another control methylglyoxal was also converted to lactic acid with strong base (Cannizzaro conditions) in  $D_2O$ . The reaction yielded lactic acid with the characteristic  $^1H$  NMR signals at 1.315 (3 H, d,  $J = 6.9$  Hz, peaks at 1.279 and 1.348 ppm) and 4.098 ppm (1 H, q,  $J = 6.9$  Hz). This experiment thus reconfirmed that the intramolecular Cannizzaro reaction occurs by a hydride shift mechanism. A final control was carried out to ensure that the product lactic acid does not incorporate deuterium into the C-2 position, even in strong basic solutions (KOH- $D_2O$ ).

Previously, Franzen described the intramolecular rearrangement of the hemithiol acetal **6** of phenylglyoxal (**1b**) and



*N,N*-diethylcysteamine (**5**) to the corresponding thiol ester in  $D_2O$ .<sup>8</sup> Since no deuterium incorporation was detected by IR in the product mandelic acid (**4b**), it was proposed that the mechanism of the rearrangement proceeded via a 1,2-hydride shift. Since we had not previously observed the expected IR absorption bands for  $[2\text{-}^2H]$ lactic and  $[2\text{-}^2H]$ mandelic acid derivatives,<sup>9</sup> we decided to repeat Franzen's earlier work. However, we would use  $[1\text{-}^2H]$ phenylglyoxal and *N,N*-diethylcysteamine in aqueous solution and monitor loss or retention of deuterium using high-resolution NMR and mass spectrometry. Figure 5 indicates that the mechanism of this reaction is also an enediol proton transfer, and not a 1,2-hydride shift, since the isotope label is lost to the medium. The ratio of the aromatic protons at 7.422 (5 H, s) and C-2 tertiary proton at 4.985 ppm (1 H, s) was ca. 5:1 indicating the incorporation of solvent protons to be ca. 100% in the product mandelic acid (**4b**).

## Conclusion

It has been previously demonstrated that the mechanism of glyoxalase I proceeds by an enediol proton transfer mechanism<sup>2a</sup> and this study now demonstrates that the essential catalytic components of the enzyme, glutathione, a base, and magnesium ion, also provide a model catalytic system. The role of glutathione is that of a covalent catalyst that by forming the covalently bonded intermediate **2** renders the former aldehydic proton now acidic, a role apparently ideal for sulfur.<sup>19</sup> A basic amino acid residue<sup>7</sup> at the active site, functioning as a general base catalyst, removes this acidic proton. The major role of the magnesium ion, if important in catalysis, may be that of chelating the substrate **2** to the enzyme surface at the active site.<sup>12,17b</sup>

## Experimental Section

Infrared spectra were determined with a Beckman Model IR-10 infrared recording spectrophotometer. Ultraviolet spectra were determined with a Cary Model 14 or Beckman Model Acta III recording spectrophotometer equipped with a thermostated cell compartment ( $30.0 \pm 0.1$  °C). The  $^1H$  NMR spectra were determined at 100 MHz using a JEOL Model JNM-PS-FT-100 fast Fourier transform NMR spectrometer (25 transients using a 90 ° pulse, 8K data points, 625–1000 Hz spectral width). The NMR chemical shifts, which are reproducible to  $\pm 0.003$  ppm, are expressed in  $\delta$  values (parts per million) relative to an  $\text{Me}_4\text{Si}$  internal standard when using  $\text{CDCl}_3$  or relative to DSS (sodium 4,4-dimethyl-4-silapentanesulfonate) when using  $D_2O$  (99.8%). All pH measurements were determined with a

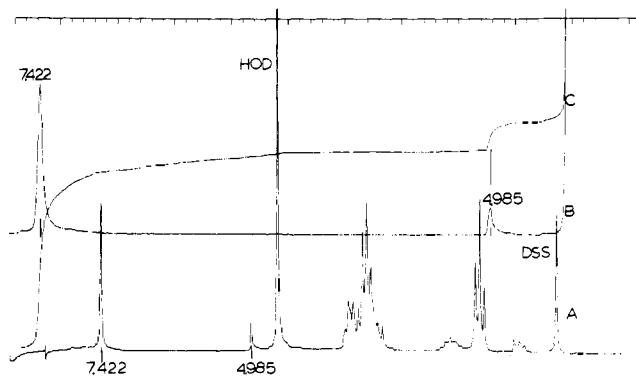


**Figure 5.**  $^1H$  NMR spectrum for the *N,N*-diethylcysteamine catalyzed conversion of  $[1\text{-}^2H]$ phenylglyoxal to mandelic acid in  $H_2O$ . Chemical shifts are quoted in parts per million from DSS. The unassigned peaks belong to the catalyst. A is the entire spectrum; B is an expansion of the 4.5–8.0 ppm region of A; C is an integration of B.

Radiometer/Copenhagen Model PHM62 pH meter equipped with a Radiometer combination Model GK2301C single electrode. Column chromatography was accomplished on 60–200 mesh silica gel (Grace, grade 62). Dioxane was distilled just prior to use from sodium.  $[^2H_6]$ Acetone (minimum 99.5%  $^2H$ ) was from Wilmad Glass Co. and  $[^2H_3]$ acetophenone was from Merck & Co., Inc. Methylglyoxal and phenylglyoxal were from Aldrich Chemical Co.  $\text{NaBH}_4$  and  $\text{NaBD}_4$  were obtained from Ventron Corp. (Alfa Products). All other chemicals were reagent grade from Fisher Scientific Co.

Phenylglyoxal hydrate was purified by repeated recrystallizations using a previously described technique<sup>10</sup> yielding white needles, mp 87–87.5 °C. Methylglyoxal hydrate (40% aqueous solution) was distilled, bp 90–100 °C (760 Torr), and then the acidic impurities removed by passing the diluted distillate through a Dowex-1 ( $\text{OH}^-$  form) ion exchange column. Dilute stock solutions were stored cold and standardized using a semicarbazide procedure<sup>20</sup> just prior to use.

**$[1\text{-}^2H, 3\text{-}^2H_3]$ Methylglyoxal Hydrate.**<sup>15,21</sup> To a solution of 3.30 g (51.5 mmol) of  $[^2H_6]$ acetone in 5 mL of dioxane was added 2.75 g (21.3 mmol) of selenic acid and the mixture was heated at ca. 60 °C for 3 h. Distillation of this mixture yielded  $[1\text{-}^2H, 3\text{-}^2H_3]$ methylglyoxal hydrate (17%): bp 89–92 °C (760 Torr); IR 1720  $\text{cm}^{-1}$ ; UV of bis-(semicarbazone)<sup>20</sup>  $\lambda_{\text{max}}$  286;  $^1H$  NMR ( $D_2O$ ) indicated no signals at  $\delta$  4.81 and 5.27 ppm that are characteristic of the aldehydic proton of the mono- and dihydrate forms of methylglyoxal.<sup>2a</sup>

**$[1\text{-}^2H]$ Phenylglyoxal.**<sup>15,21</sup> To a solution of 2.00 g (16.2 mmol) of  $[^2H_3]$ acetophenone in 10 mL of dioxane was added 1.30 g (10.0 mmol) of selenic acid and the mixture was gently refluxed for 1 h. The reaction mixture was then partitioned between ether and an aqueous layer saturated with  $\text{Na}_2\text{CO}_3$ , KCl, and NaCl. The organic layer was dried ( $\text{Na}_2\text{SO}_4$ ) and concentrated in vacuo, and the residue chromatographed (silica gel). Elution with ether–petroleum ether yielded  $[1\text{-}^2H]$ phenylglyoxal (63%): IR 1716, 1698, and 1674  $\text{cm}^{-1}$ ;<sup>22</sup> UV  $\lambda_{\text{max}}$  249.5 ( $\epsilon$  10 300);<sup>10</sup>  $^1H$  NMR ( $D_2O$ )  $\delta$  7.61 and 8.07 ppm (phenyl multiplets).

**$[2\text{-}^2H]$ Lactic Acid (and Lactic Acid).** To a stirred slurry of 110 mg (1.0 mmol) of sodium pyruvate in 2 mL of methanol was added 12 mg (0.29 mmol) of  $\text{NaBD}_4$ . Once the slurry dissolved (ca. 4 min), ca. 7 drops of 5% HCl was added and then after 15 min the reaction mixture lyophilized. The residue was dissolved in 1 mL of  $D_2O$  (2 mg of DSS):  $^1H$  NMR  $\delta$  1.309 ppm (s,  $\text{CH}_3$ ).

Lactic acid was prepared in the same manner using  $\text{NaBH}_4$ :  $^1H$  NMR  $\delta$  1.315 (3 H, d,  $J = 6.9$  Hz, peaks at 1.279 and 1.348 ppm) and 4.098 ppm (1 H, q,  $J = 6.9$  Hz). The  $^1H$  NMR spectrum was identical with an authentic sample of lactic acid.

**Kinetics. Thiol Ester Procedure.**<sup>13a</sup> The model reactions generally contained 1–2 mM GSH, 5–10 mM methylglyoxal, and 0.02–0.8 M buffer at neutral pH. The reaction rate was measured by following the increase in absorption maximum of the thiol ester at 240 nm ( $\epsilon$  3370) at  $30.1 \pm 0.1$  °C.

**Semicarbazide Procedure.**<sup>20</sup> Aliquots (25–80  $\mu\text{L}$ ) from the model reactions ( $30.0 \pm 0.1$  °C) were periodically taken and immediately

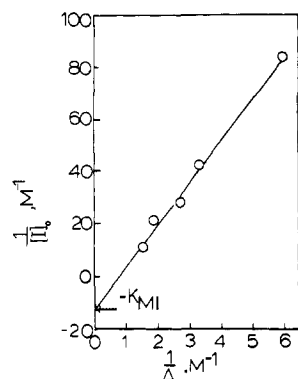


Figure 6. Determination of the methylglyoxal-imidazole association constant.

quenched in 10.0 mL of a 0.1 M (pH 7.00) phosphate buffer solution containing 0.150 M semicarbazide-HCl. To ensure quantitative conversion of unreacted methylglyoxal to the bis(semicarbazone), these mixtures were allowed to react for ca. 10 h at ambient temperature. The reaction rate was then calculated by determining the disappearance of methylglyoxal with time by measuring the absorption maximum of the methylglyoxal bis(semicarbazone) at 286 nm ( $\epsilon = 32\,000$ ). At 30 °C the model reactions obeyed pseudo-first-order kinetics for at least 220 min and the semilog plots (absorbance vs. time) gave a linear regression coefficient of at least 0.999. The  $k_{\text{obsd}}$  values are obtained from these plots and represent pseudo-first-order rate constants.

**$^1\text{H}$  NMR Solvent Incorporation Studies.** In a typical experiment, using a phosphate dianion catalyzed experiment as an example, 70 mg (0.78 mmol) of methylglyoxal<sup>2a</sup> and 200 mg (0.65 mmol) of glutathione were dissolved in 5.0 mL of  $\text{D}_2\text{O}$  (99.8%), and then the pH of the solution was adjusted to 7.00 (pD 7.40) by the addition of 362 mg (2.08 mmol) of anhydrous  $\text{K}_2\text{HPO}_4$ . The stirred solution (magnetic stirrer) was equilibrated in a thermostated circulating water bath at  $30.0 \pm 0.1$  °C. Aliquots of this reaction solution were periodically transferred to a highly polished 5-mm NMR tube containing DSS and the spectrum was recorded. Since the glutathionylthiol ester of lactic acid gives rise to a methyl signal that is downfield from that of lactate (see the Results and Discussion section),  $^1\text{H}$  NMR spectroscopy can be used to detect the presence of both products in the same reaction mixture. The general bases employed in this study catalyzed the conversion of the hemithiol acetal **2a** to the thiol ester **3a** and then slowly hydrolyzed the thiol ester **3a** to lactic acid. The hydrolysis was usually complete within ca. 4 days and could be confirmed by adding solid KOH to the NMR tube and observing no further change in the spectrum in the 1.2–1.5-ppm region.

The control experiments that established that *S*-lactoylglutathione **3a** does not incorporate solvent protons when exposed to the reaction conditions are exactly those previously described on p 7461 of ref 2a except that no glyoxalase II was subsequently added. The reaction mixture was monitored by 100-MHz NMR for 4 days.

**Acknowledgment.** The authors wish to thank the National Cancer Institute (National Institutes of Health), the Charles and Johanna Busch Memorial Fund (Rutgers University), the Research Council (Rutgers University), the National Institutes of Health (Biomedical Sciences Support Grant), and Mrs. Lauretta Horstmann, Bagley, Wis., for grants supporting our enzyme studies.

## Appendix

**Determination of Association Constant for Methylglyoxal and Imidazole.** Equilibrium solutions of methylglyoxal (M) and imidazole (I) at constant pH (7.00), ionic strength (0.40, KCl), and temperature (30 °C) were studied by UV spectroscopy at 280 nm. Data for  $2.87 \times 10^{-3}$  M methylglyoxal solutions containing increasing amounts of imidazole are presented in Table I. Assuming that at equilibrium all three components are contributing to the optical density, the ob-

Table I. UV Spectroscopic Data Employed in the Determination of the Methylglyoxal-Imidazole Association Constant<sup>a</sup>

run	[imidazole], M	OD <sub>280</sub>	$\Delta\text{OD}$
1		0.301	
2	0.0119	0.421	0.120
3	0.0238	0.538	0.237
4	0.0358	0.650	0.349
5	0.0473	0.766	0.465
6	0.0946	1.194	0.893

<sup>a</sup> At 30 °C, pH 7.00, ionic strength of 0.4, and an initial methylglyoxal concentration of  $2.87 \times 10^{-3}$  M.

served OD<sub>280</sub> is represented by eq 7:

$$\text{OD}_{280} = \epsilon_I[I] + \epsilon_M[M] + \epsilon_{MI}[\text{MI}] \quad (7)$$

The extinction coefficients  $\epsilon_I$ ,  $\epsilon_M$ , and  $\epsilon_{MI}$ , at 280 nm (1-cm cells) and equilibrium concentrations [I], [M], and [MI] are for imidazole, methylglyoxal, and the methylglyoxal-imidazole complex, respectively.  $\epsilon_I$  was determined to be 8.83. Employing the mass balance equations, eq 7 becomes eq 8:

$$\text{OD} = \epsilon_I([I]_0 - [\text{MI}]) + \epsilon_M([M]_0 - [\text{MI}]) + \epsilon_{MI}[\text{MI}] \quad (8)$$

The difference in optical density ( $\Delta\text{OD}$ ) between the first run and any other is expressed by eq 9:

$$\Delta\text{OD} = \epsilon_I\Delta[I]_0 + (\epsilon_{MI} - \epsilon_I - \epsilon_M)\Delta[\text{MI}] \quad (9)$$

Since all observations are compared to run no. 1 with no added imidazole ( $[I]_0 = 0$ ), then  $\Delta[I]_0 = [I]_0$  for any run and  $\Delta[\text{MI}] = [\text{MI}]$ . Rearranging eq 9 yields eq 10

$$[\text{MI}] = \frac{\Delta\text{OD} - \epsilon_I[I]_0}{\epsilon_{MI} - \epsilon_I - \epsilon_M} = \frac{\Delta}{\epsilon_T} \quad (10)$$

where  $\Delta = \Delta\text{OD}/\epsilon_I - [I]_0$  and  $\epsilon_T = (\epsilon_{MI} - \epsilon_I - \epsilon_M)/\epsilon_I$ . Assuming a 1:1 complex between methylglyoxal and imidazole, the equilibrium constant is given in eq 11:

$$K_{MI} = \frac{[\text{MI}]}{[I][M]} = \frac{[\text{MI}]}{([I]_0 - [\text{MI}])([M]_0 - [\text{MI}])} \quad (11)$$

Substituting  $\Delta/\epsilon_T$  for [MI] and assuming  $[I]_0 \sim [I]$ , which is valid when  $[I]_0 \gg [M]_0$ , then

$$K_{MI} = \frac{\Delta}{\epsilon_T[I]_0([M]_0 - \Delta/\epsilon_T)} \quad (12)$$

Equation 12 can be rearranged to a double reciprocal plot (eq 13):

$$\frac{1}{\Delta}\epsilon_T[M]_0K_{MI} - K_{MI} = \frac{1}{[I]_0} \quad (13)$$

As can be seen from Figure 6, a plot of  $1/\Delta$  vs.  $1/[I]_0$  is indeed linear with a  $K_{MI} = 12.9 \pm 2.3 \text{ M}^{-1}$ .

## References and Notes

- (1) This investigation was supported primarily by Public Health Service Research Grant No. CA 12984 from the National Cancer Institute.
- (2) (a) Part 2: S. S. Hall, A. M. Doweiko, and F. Jordan, *J. Am. Chem. Soc.*, **98**, 7460 (1976); (b) part 3: S. S. Hall, L. M. Doweiko, A. M. Doweiko, and J. S. R. Zilenovski, *J. Med. Chem.*, **20**, 1239 (1977).
- (3) Abstracted from the Ph.D. Dissertation of A. M. Doweiko, 1975.
- (4) (a) A. Szent-Györgyi, L. G. Együd, and J. A. McLaughlin, *Science*, **155**, 539 (1967); (b) L. G. Együd, J. A. McLaughlin, and A. Szent-Györgyi, *Proc. Natl. Acad. Sci. U.S.A.*, **57**, 1422 (1967); (c) R. Vince and W. B. Wadd, *Biochem. Biophys. Res. Commun.*, **35**, 593 (1969); (d) R. Vince and S. Daluge, *J. Med. Chem.*, **14**, 35 (1971).
- (5) V. Franzen, *Chem. Ber.*, **89**, 1020 (1956).
- (6) I. A. Rose, *Biochim. Biophys. Acta*, **25**, 214 (1957).
- (7) Histidine modification (unpublished from this laboratory) inactivates yeast glyoxalase I, suggesting that histidine may serve as the general base catalyst for the enzyme.
- (8) (a) V. Franzen, *Chem. Ber.*, **88**, 1361 (1955); (b) *Ibid.*, **90**, 623 (1957).
- (9) (a) S. S. Hall and A. Poet, *Tetrahedron Lett.*, 2867 (1970). (b) These experiments were all carried out at 30 °C and at pH 6.6 with a solution that

- contained 0.05 M imidazole, 0.0052 M GSH, 0.026 M methylglyoxal, and for this specific rate enhancement 0.052 M MgCl<sub>2</sub> and 0.185 M KCl (ionic strength of 0.4).
- (10) J. Hine and G. F. Koser, *J. Org. Chem.*, **36**, 3591 (1971).
- (11) J. Hine and C. D. Fischer, Jr., *J. Am. Chem. Soc.*, **97**, 6513 (1975).
- (12) K. A. Davis and G. R. Williams, *Biochim. Biophys. Acta*, **113**, 393 (1966).
- (13) (a) E. Racker, *J. Biol. Chem.*, **190**, 685 (1951); (b) D. L. Vander Jagt and L.-P. B. Han, *Biochemistry*, **12**, 5161 (1973).
- (14) E. J. Cohn and J. T. Edsall, "Proteins, Amino Acids, and Peptides as Ions and Dipolar Ions", Reinhold, New York, N.Y., 1943, p 445.
- (15) D. L. Vander Jagt, L.-P. B. Han, and C. H. Lehman, *Biochemistry*, **11**, 3735 (1972).
- (16) The larger  $k_B$  for HPO<sub>4</sub><sup>2-</sup> than for imidazole is due to two equivalent base sites in the former and only one in the latter.
- (17) (a) L.-P. B. Han, L. M. Davison, and D. L. Vander Jagt, *Biochim. Biophys. Acta*, **445**, 486 (1976); (b) L.-P. B. Han, C. M. Schmandle, L. M. Davison, and D. L. Vander Jagt, *Biochemistry*, **16**, 5478 (1977).
- (18) P. F. Leadlay, W. J. Albery, and J. R. Knowles, *Biochemistry*, **15**, 6517 (1976).
- (19) (a) A. I. Shatenshtein and H. A. Guozdeva, *Tetrahedron*, **25**, 2749 (1969); (b) A. Streltweiser and J. E. Williams, *J. Am. Chem. Soc.*, **97**, 191 (1975); (c) F. Bernardi, I. G. Csizmadia, A. Mangini, H. B. Schlegel, M.-H. Whangbo, and S. Wolfe, *ibid.*, **97**, 2209 (1975); (d) F. G. Bordwell, M. Van Der Puy, and N. R. Vanler, *J. Org. Chem.*, **41**, 1885 (1976).
- (20) N. M. Alexander and J. L. Boyer, *Anal. Biochem.*, **41**, 29 (1971).
- (21) H. L. Riley, J. F. Morley, and N. A. C. Friend, *J. Chem. Soc.*, 1875 (1932).
- (22) D. L. Vander Jagt, L.-P. B. Han, and C. H. Lehman, *J. Org. Chem.*, **37**, 4100 (1972).

## Resonance Raman Spectra of Copper-Sulfur Complexes and the Blue Copper Protein Question

Nancy S. Ferris,<sup>1a</sup> William H. Woodruff,<sup>\*1a</sup> David B. Rorabacher,<sup>1b</sup> T. E. Jones,<sup>1b</sup> and L. A. Ochrymowycz<sup>1c</sup>

Contribution from the Departments of Chemistry, University of Texas at Austin, Austin, Texas 78712, Wayne State University, Detroit, Michigan 48202, and the University of Wisconsin at Eau Claire, Eau Claire, Wisconsin 54701. Received January 24, 1977

**Abstract:** Resonance Raman spectra are reported for copper(II) complexes of thiaether and mercaptide ligands. The copper-sulfur stretching frequencies in the complexes are compared to those reported by previous workers for the blue copper proteins. The vibrational results strongly suggest that methionine sulfur is bound to copper in the proteins. In the case of stellacyanin, which contains no methionine, a Cu-S (disulfide) bond is suggested. The resonance Raman intensity pattern for one of the thiaether complexes is interpreted using a single-state resonance expression and an expression involving vibronic coupling and two-state resonance. The results, together with the observed intensity of the assigned copper-(methionine) sulfur vibration in the proteins, suggest possible resonance mechanisms for this low-intensity vibration, and details of the electronic assignments for the copper-(methionine) sulfur charge-transfer transitions.

Blue copper proteins, in addition to their essential biological functions, are characterized by a series of curious spectroscopic and chemical properties.<sup>2</sup> The question of the nature of the copper coordination environment in the proteins, which is responsible for these unique properties, is a matter of considerable interest. A central feature of many suggested structures of the blue copper environment is the presence, in addition to the more usual nitrogen and/or oxygen ligands, of a copper-sulfur bond.<sup>3-8</sup> Copper-sulfur bonding in these proteins is consistent with a large body of spectroscopic and chemical evidence.<sup>4-7,9-11</sup> Until very recently,<sup>16</sup> however, the identity of the sulfur ligand had not been established.<sup>9,12-15</sup>

Based upon electronic spectra and chemical evidence on copper thiaether complexes,<sup>17</sup> methionine has been suggested as a possible ligand for copper in the blue proteins. Later, the same suggestion was advanced<sup>8</sup> on the basis of the amino acid sequences of plastocyanin and azurin. The possibility of methionine binding has, however, generally been dismissed (see ref 18 and references therein), in favor of the more commonly accepted cysteine sulfur coordination.<sup>3-7</sup> It was thought by most workers, with the exception of one,<sup>8</sup> that *either* cysteine *or* methionine, but not both, was bound to copper in the proteins.<sup>3-7,9-15,17</sup>

The resonance Raman technique<sup>19</sup> has been applied to blue copper proteins,<sup>5,6</sup> and a copper-sulfur stretching frequency has been assigned to several of these systems. However, no vibrational data concerning copper bound to sp<sup>3</sup> sulfur (of the thiaether or mercaptide types found in proteins) was available to aid in evaluating the protein vibrational results. (Recently, the resonance Raman spectrum of a complex wherein Cu(II) is bound to mercaptide sulfur has been reported.<sup>20</sup>) We have

applied the resonance Raman technique to copper mercaptide<sup>21</sup> and thiaether<sup>17</sup> complexes which have previously been suggested on the basis of ESR,<sup>21</sup> electronic absorption,<sup>17</sup> and redox<sup>17</sup> evidence as possible analogues of the copper-sulfur binding in the blue copper proteins. Our results constitute the first vibrational study of complexes in which Cu(II) is bound to thiaether and mercaptide sulfur. The resonance Raman evidence suggests that methionine or a similar neutral sulfur ligand such as disulfide is coordinated to copper in all of the blue proteins. Stellacyanin alone contains no methionine,<sup>9,29</sup> and therefore is unique in that it must employ one of the alternate "methionine-like" ligands.

The resonance Raman evidence for methionine binding was presented in the original and subsequent revisions of this paper. The copper ligands in plastocyanin have since been determined by X-ray structural analysis.<sup>16</sup> This structural determination shows that two histidine nitrogens, a cysteine sulfur, and a methionine sulfur are bound to copper in plastocyanin. Thus, unexpectedly, both previously suggested modes of copper-sulfur binding at the blue copper site actually occur, at least in plastocyanin. Despite the structural determination on plastocyanin and other crystallographic work in progress, spectroscopic evidence will continue to be important in inferring the nature of the copper environment in the remaining blue proteins, some of which may never be crystallized.

### Experimental Section

The copper mercaptide and polythiaether complexes were prepared using previously described procedures.<sup>17,21</sup> The BF<sub>4</sub><sup>-</sup> salt of the Cu(II) complex of 2,6-bis(methylthiomethyl)pyridine<sup>22</sup> (SNS) was obtained from Dr. P. S. Bryan and the Cu(II) complex of 2,2'-bis(2-benzim-